Published in final edited form as:
Exp Cell Res. 2013 November 15; 319(19): . doi:10.1016/j.yexcr.2013.09.007.

Bone Marrow-Derived Mesenchymal Stem Cells Enhance Angiogenesis via their α6β1 Integrin Receptor

Bita Carrion[a], **Yen P. Kong**[a], **Darnell Kaigler**[a,b], and **Andrew J Putnam**[a,1]

[a]Department of Biomedical Engineering, University of Michigan; Ann Arbor, MI 48109

[b]Department of Periodontics and Oral Medicine, University of Michigan; Ann Arbor, MI 48109

Abstract

Bone marrow-derived mesenchymal stem cells (BMSCs) facilitate the angiogenic response of endothelial cells (ECs) within three-dimensional (3D) matrices *in vivo* and in engineered tissues *in vitro* in part through paracrine mediators and by acting as stabilizing pericytes. However, the molecular interactions between BMSCs and nascent tubules during the process of angiogenesis are not fully understood. In this study, we have used a tractable 3D co-culture model to explore the functional role of the α6β1 integrin adhesion receptor on BMSCs in sprouting angiogenesis. We report that knockdown of the α6 integrin subunit in BMSCs significantly reduces capillary sprouting, and causes their failure to associate with the nascent vessels. Furthermore, we demonstrate that the BMSCs with attenuated α6 integrin proliferate at a significantly lower rate relative to either control cells expressing non-targeting shRNA or wild type BMSCs; however, despite adding more cells to compensate for this deficit in proliferation, deficient sprouting persists. Collectively, our findings demonstrate that the α6 integrin subunit in BMSCs is important for their ability to stimulate vessel morphogenesis. This conclusion may have important implications in the optimization of cell-based strategies to promote angiogenesis.

Keywords

Angiogenesis; Mesenchymal stem cell; α6β1 integrin; Microenvironment; Fibrin

Introduction

Strategies to vascularize implanted cell-scaffold constructs are the focus of many attempts to engineer viable, functional tissues. One approach to overcoming this challenge is to incorporate penetrating vascular networks within tissue constructs *in vitro*, which in turn can successfully integrate with the host vasculature upon implantation *in vivo* [1, 2]. However, engineering capillary networks with the functional properties of native vascular networks, including the abilities to deliver oxygen and nutrients and regulate permeability, have been difficult to generate in tissue engineered constructs. In the past 10–20 years, it has been widely recognized that cells of a mesenchymal origin greatly contribute to the development and stabilization of the microvasculature, in part by acting as stabilizing pericytes

[1]Corresponding author: Andrew J. Putnam, Ph.D., Department of Biomedical Engineering, University of Michigan, 2154 Lurie Biomedical Engineering Building, 1101 Beal Ave, Ann Arbor, MI 48109, Phone: (734) 615-1398, Fax: (734) 647-4834, putnam@umich.edu.

characterized by the expression of markers such as α-smooth muscle actin (αSMA) and neuron-glial antigen 2 (NG2) [3, 4]. However, the molecular mechanisms by which these cells influence capillary morphogenesis remain unresolved.

Angiogenesis, a process crucial to the growth and maintenance of tissues, represents the emergence of new pericyte-invested capillary blood vessels from pre-existing vasculature [5]. Nascent capillaries branch from existing ones via leading endothelial tip cells, and are subsequently stabilized by pericytes during the later stages of angiogenesis to yield a mature vascular network composed of non-leaky blood vessels [5–7]. Pericytes are thought to be derived from multilineage progenitor cells that exhibit the features of MSCs [3], and intimately associate with the ECs in newly developed capillaries in part through their shared basement membrane [8, 9]. Our group has previously demonstrated that different stromal cells, including BMSCs, enhance angiogenesis via distinct mechanisms that impact the functional qualities of the capillary networks both *in vitro* [10] and *in vivo* [11]. Understanding the mechanisms by which different populations of stromal cells co-delivered with ECs regulate vascular morphogenesis will be essential to optimize strategies to promote vessel formation and maturation in engineered tissues.

BMSCs are non-hematopoietic cells found in the adult bone marrow that have been shown to possess multipotency [12–14]. BMSCs are also found in a perivascular niche adjacent to blood vessels [3, 15], an anatomic location common to other adult stem cell populations, including adult neural stem cells (NSCs) [16–18], adipose-derived stem cells [3], and hematopoietic stem cells [19]. In addition to their multilineage characteristics, BMSCs are capable of promoting angiogenesis [20–22], making these cells particularly attractive for engineering vascularized tissues. When co-cultured with ECs within a 3D matrix *in vitro*, BMSCs stimulate a strong angiogenic response and adopt a pericytic phenotype localized subjacent to the developed capillary networks [23]. While some aspects of the mechanisms by which BMSCs induce ECs to form capillaries have been elucidated [24, 25], many details of these mechanisms remain unknown.

In this present study, we have adapted an established 3D co-culture model of sprouting angiogenesis [25–27] to investigate the interaction between α6β1 integrin expressed in BMSCs and EC-derived laminin-rich basement membrane [28]. Prior studies with NSCs have shown that their interaction with capillaries occurs in part through the binding of this integrin to EC-deposited laminin, and that this interaction is critical for maintaining their quiescence [17]. Given the common perivascular location of both BMSCs and NSCs, we hypothesized that the α6β1 integrin-laminin interaction is essential for BMSCs to adopt a perivascular location, and that this interaction is important for their ability to promote angiogenesis. We show here that knockdown of the α6 integrin subunit in BMSCs results in a significant decrease in the ability of ECs to form capillary sprouts, a reduction in laminin expression in EC-BMSC co-cultures, reduced proliferation of BMSCs, and altered expression patterns of αSMA.

Materials and Methods

Cell isolation and culture

Human umbilical vein endothelial cells (HUVECs) were isolated from freshly harvested umbilical cords, as previously described [20]. Briefly, the vein was flushed with sterile phosphate buffer saline (PBS) and then incubated with 0.1% collagenase type I (Worthington Biochemical, Lakewood, NJ) for 20 minutes at 37°C. The digestion product and subsequent PBS wash were collected and centrifuged. The cell pellet was resuspended in endothelial growth medium (EGM-2, Lonza, Walkersville, MD), plated onto T-25 flasks, and allowed to attach overnight. PBS was used to wash away red blood cells the following

day. Human BMSCs (Lonza) were cultured in high glucose (4.5 g/L) Dulbecco's modified Eagle medium (DMEM, Invitrogen, Carlsbad, CA) supplemented with 10% fetal bovine serum (FBS, Invitrogen). All cultures were incubated at 37°C and 5% CO_2. Media were changed every 2 days and cells were harvested with 0.05% Trypsin-EDTA (Invitrogen). BMSCs were used prior to passage 8 and HUVECs at passage 3.

Construction of the 3D co-culture model

Construction of the 3D co-culture model was performed as described previously [21]. In brief, mCherry-transduced HUVECs were coated on 10^4 Cytodex™ microcarrier beads (Sigma-Aldrich Co., St. Louis, MO) and mixed with 5×10^4 BMSCs within a 2.5 mg/mL fibrin solution. Five hundred microliters of this solution containing ~100 HUVEC-coated beads was combined with 10 μL of thrombin (50 U/mL) in a single well of a 24-well plate to make one gel construct. This process was repeated until the desired number of gels was constructed. The gel constructs were left undisturbed for 5 min to allow the beads to settle near the bottom of the well before incubating for 25 min at 37°C and 5% CO_2 to induce gelation. Tissues were then cultured in fully supplemented EGM-2 for 7 days, with the media changed every 2 days.

Fluorescent labeling of cells for both live and fixed cell imaging

HUVECs were fluorescently tagged using the red fluorescent protein mCherry to facilitate visualization and quantification of vessel networks in some experiments. mCherry-labeling was achieved via retroviral transduction using the Phoenix Ampho Retrovirus Expression system (Orbigen, San Diego, CA), as previously described [29]. Wild type BMSCs were fluorescently labeled using a green cell tracker dye, SP-$DiOC_{18}$ (3) (Invitrogen) according to manufacturer's protocol. In other experiments, cells within 3D fibrin gels and 2D cultures were fixed and stained for fluorescent imaging at defined end points. Fixed and permeabilized cells were extensively washed with TBS-T buffer to rid of the green fluorescent protein (GFP) expressed in the cytosol of BMSCs transduced with the silencing and non-targeting shRNA plasmids, and incubated with primary antibodies overnight at 4°C. Next, appropriate secondary antibodies were incubated for 2.5 hours at 4°C. Cell nuclei were stained with DAPI, 1 μg/ml (Sigma-Aldrich, St. Louis, MO) in PBS for 10 minutes. The following antibodies were used for immunofluorescent staining: monoclonal mouse anti-human αSMA, 1:200 (Abcam, Cambridge, MA); rabbit anti-human laminin, 1:100 (Abcam); monoclonal mouse anti-α6 integrin, 1:50 (Millipore, Billerica, MA); AlexaFluor 488 goat anti-mouse IgG secondary antibody, 1:450 (Invitrogen); and AlexaFluor 594 goat anti-rabbit IgG secondary antibody, 1:450 (Invitrogen).

Knockdown of α6 integrin expression via RNA interference

The expression level of α6 integrin was attenuated by transducing BMSCs with the pGIPZ lentiviral shRNA (Open Biosystems, Rockford, IL) specific for the ITGA6 gene. A lentiviral shRNA plasmid against ITGA6 (5'TGCTGTTGACAGTGAGCGCTTG-GTTTTAAGTACAACTGAATAGTGAAGCCACAGATGTATTCAGTTGTACTTAAAA CCAA-ATGCCTACTGCCTCGGA-3′), and a non-targeting control (5′-TGCTGTTGACAGTG-AGCGATCTCGCTTGGGCGAGAGTAAGTAGTGAAGCCACAGATGTACTTACTCTC GCCCAAGCGAGAGTGCCTACTGCCTCGGA-3′) were separately packaged into viruses by co-transfecting them with psPAX2 (Addgene plasmid 12260) and plp-VSVG (Invitrogen) in 293FT cells (Invitrogen) using Lipofectamine 2000 (Invitrogen). After a 48-hour incubation period, the lentiviral supernatant was collected. BMSCs were incubated in DMEM supplemented with polybrene (Invitrogen) (5 μg/mL) for 15 minutes at 37°C prior to the addition of the lentiviral supernatant, and then cultured with the lentiviral supernatant for 12 hours. The lentiviral medium was removed after 48 hours and replaced by fresh

DMEM. Selection of shRNA-expressing BMSCs was achieved by culturing transduced cells in the presence of 1 μg/mL puromycin (Sigma-Aldrich) for a period of 4–6 days. BMSCs transduced with the pGIPZ constructs will also express eGFP.

Reverse transcription and quantitative polymerase chain reaction

Quantitative real time PCR was used to assess the expression levels of ITGA6 in BMSCs following shRNA-mediated silencing. Total RNA was isolated from BMSCs using the SV Total RNA Isolation System (Promega, Madison, WI). The RNA concentration and purity of each sample were determined by A260/A280 absorptions using a Nanodrop ND-1000 spectrophotometer (Thermo Scientific, Wilmington, DE). Equal amounts of total RNA from each sample were used to produce the first strand cDNA using the ImProm-II Reverse Transcription System (Promega). Taqman Gene Expression Assays (Applied Biosystems, Carlsbad, CA) were used to measure the transcript levels of the selected genes. The PCR amplification was performed on a 7500 Fast Real-Time PCR System (Applied Biosystems) in a final volume of 20 μl using cycling parameters (2 min, 50°C; 10 min, 95°C; 15 sec, 95°C; 1 min, 60°C with the latter two steps repeated for 40 times). Each reaction was performed in triplicates and the ΔΔCt method was used for the gene expression analysis. [30]

Retrieving cells from 3D fibrin gel constructs

To retrieve cells from 3D cultures, fibrin gels were degraded with nattokinase (Japan Bio Science Laboratory Co., Ltd., Osaka, Japan), a *Bacillus*-derived serine protease that is known for its potent fibrinolytic activity, as previously described [31]. Briefly, a fibrinolytic solution was prepared by dissolving 50 FU/mL (fibrin degradation unit) of nattokinase in PBS containing 1 mM EDTA (Fisher). Gels were washed with PBS before dislodging them from the well siding using a small spatula. Gels were subsequently dissolved by adding 500 μl of the fibrinolytic solution and incubating at 37°C for 30 min. Upon dissolution, the contents of each well were collected and centrifuged. Cells were then washed with cold PBS for additional procedures.

Quantification of αSMA protein expression via fluorescent activated cell sorting (FACS)

The expression levels of αSMA in the BMSCs were assessed using FACS. Cells were retrieved from 3D HUVEC-BMSC co-cultures using the nattokinase-based fibrinolytic solution described above. Retrieved HUVEC-BMSC mixtures along with beads were strained through a 40 μm cell strainer (BD Falcon, Franklin Lakes, NJ) to ensure single cellularity and remove the beads. For FACS, fixed and permeabilized cells were extensively washed with TBS-T buffer, pelleted by centrifugation at 2000 rpm at 4°C for 5 minutes, and resuspended in ice cold PBS containing 0.1–0.5% bovine serum albumin (BSA, Sigma-Aldrich). Resuspended cells were incubated with a mouse anti-α-smooth muscle actin (αSMA) monoclonal antibody (Abcam; 1:200) and rabbit anti-human CD31 antibody (Santa Cruz Biotechnologies, Santa Cruz, CA; 1:50) for 1 hour at 4°C. Samples were then washed with cold PBS containing 0.5% BSA, and incubated with AlexaFluor 633 goat anti-mouse IgG (Invitrogen; 1:450) and AlexaFluor 488 goat anti-rabbit IgG (Invitrogen; 1:450) secondary antibodies for 30–40 minutes at 4°C. As a negative control, parallel cell suspensions were prepared, and incubated with only the secondary antibodies; Samples were then washed twice and resuspended in 0.5% BSA in PBS. Flow cytometry analyses were performed on samples using a FACSAria II cell sorter (BD Biosciences, San Jose, CA) located at the Flow Cytometry Core of the University of Michigan Medical School. The percentage of BMSCs expressing αSMA (αSMA+) was obtained by dividing the number of cells expressing αSMA (αSMA+) by the total number of BMSCs. The latter number was determined via FACS based on the total number of cells that did not express CD31 (to ensure that HUVECs were not included in the total denominator).

Western blotting for αSMA and laminin

For Western blotting, cells were retrieved from 3D HUVEC-BMSC co-cultures using the nattokinase-based fibrinolytic solution described above, and subsequently lysed in Garner buffer (50mM Tris, pH 7.5; 150mM NaCl; 1mM phenylmethylsulfonyl fluoride; 1% Triton X-100). The lysate was clarified by centrifugation at 14,000 rpm and 4°C for 10 minutes. The supernatant was collected and total protein concentration was determined. After boiling, equal amounts of total protein from lysates were loaded into Novex tris-glycine gels (Invitrogen) and subjected to SDS-PAGE. For αSMA, 10% gels were used; for laminin, 4–12% gradient gels were used. The separated proteins were then transferred onto a poly(vinylidene fluoride) membrane and probed with either a mouse monoclonal anti-human αSMA antibody (1:200, Abcam) or a rabbit polycloncal anti-pan-laminin antibody (1:100, Abcam). After washing, the membranes were incubated with horseradish peroxidase-conjugated secondary antibodies (Santa Cruz Biotechnologies) of the species appropriate for each primary. Protein expression was visualized using an enhanced chemiluminescence detection system.

Quantification of total network lengths

To quantitatively assess capillary morphogenesis, total network lengths were measured in the 3D co-culture model of angiogenesis as previously described [29]. Briefly, capillary networks formed by mCherry transduced HUVECs in the presence of BMSCs were imaged at three time points post assembly (Day 1, 3, and 7) via fluorescent microscopy (Olympus IX81, Olympus America, Center Valley, PA). A total of 10 beads per condition were imaged at low magnification (4x), and tracked longitudinally across all time points. Total vessel network lengths per bead were measured using the Angiogenesis Tube Formation module within MetaMorph Premier Software (Molecular Devices, Sunnyvale, CA).

Cell proliferation assay

To assess the influence of ITGA6 knockdown on BMSC proliferation, BMSCs grown in mono-culture in 3D fibrin gels or in co-culture with HUVECs were retrieved using nattokinase as described above. The total DNA content of the cells retrieved from the 3D fibrin gels after 1, 3, and 7 days of culture was quantified using a commercially available DNA assay (PicoGreen, Invitrogen) according to the manufacturer's instructions.

Adhesion blocking assay

To complement qPCR, silencing of the ITGA6 gene in BMSCs was functionally confirmed using a standard cell adhesion assays, similar to that previously described [23]. The relative adhesive properties of ITGA6 knock-down BMSCs to laminin were compared to those of wild-type BMSCs and BMSCs transduced with the shNT control vector. Mouse laminin (Invitrogen) was covalently attached to tissue culture plastic using the sulfo-SANPAH hetero-bifunctional linker (Proteochem, Inc., Denver, CO). Briefly, 0.5 mM of sulfo-SANPAH was dissolved in 0.1 M MES (Fisher), 0.5 M NaCl (Fisher), pH 6.0 buffer and placed into the wells of an untreated 96-well tissue culture plates (Nunc, Thermo Scientific). The sulfo-SANPAH solution was then irradiated with UV light for 15 minutes and removed by rinsing with MES buffer. This step was repeated with fresh sulfo-SANPAH and rinsed with MES buffer. Laminin (100 μg/mL) was prepared in PBS, pH 7.0 and added to the sulfo-SANPAH functionalized wells and incubated overnight at 4°C. The wells were rinsed with PBS the next day. The next day, BMSCs (3×10^5 cells/mL) were pre-incubated in serum-free DMEM for 15 min. The wells of the 96-well plate were rinsed with PBS; then 0.1 mL of the cell suspension was added to each well. Cells were incubated at 37°C for 1 h, at which point non-adherent cells were washed away. The attached cells were fixed and stained with a 0.4% crystal violet in methanol (w/v) for 30 min. After washing with distilled

water, the stain was extracted with 0.1 M citrate in 50% ethanol. The absorbance of each well of the plates was measured at 590 nm with a Multiskan Spectrum microplate reader (Thermo Fisher Scientific).

Statistical Analysis

Statistical analysis was carried out using GraphPad Prism software. Data are reported as means ± standard deviations. All statistical comparisons were made by performing a two-way analysis of variance (ANOVA), followed by Bonferroni's multiple comparison tests to judge significance between two data sets at a time. *P* values less than 0.05 were considered statistically significant.

Results

BMSCs stimulate HUVECs to form robust capillary networks when co-cultured within 3D fibrin gels

In prior studies, we have demonstrated that BMSCs are capable of inducing HUVECs to undergo capillary morphogenesis *in vitro* [24, 25] and *in vivo* [11, 32]. First, we confirmed these earlier observations, showing that BMSCs induced HUVECs to form vascular networks (Fig. 1). In this model system, HUVECs coated on microcarrier beads sprout and extend through the surrounding 3D fibrin ECM over a period of time. To monitor vessel growth, fluorescent microscopy was used to trace the HUVECs transduced with mCherry (Fig. 1A, D, G), while wild type BMSCs were fluorescently labeled using a green cell tracker dye (Fig.1B, E, H) in order to qualitatively differentiate capillary networks from the presence of surrounding stroma. After validating the use of this 3D fibrin-based *in vitro* model for studying BMSC-induced angiogenesis, we subsequently utilized this system to address the role of BMSC α6 integrin in this process.

Knockdown of α6 integrin subunit expression in BMSCs diminishes vessel sprouting

We hypothesized that the BMSCs' α6β1 integrin receptor is important for their ability to stimulate angiogenesis. This hypothesis arose from the fact that some progenitor populations interact with capillaries in part via their α6β1 integrin receptor and EC-deposited laminin [17, 23]. To investigate a role for this integrin in BMSC-induced angiogenic sprouting, we knocked down its expression levels via RNA interference, achieving a reduction in expression levels of 82% (relative to the shNT controls) as measured by qPCR (Fig. 2A). Immunofluorescent labeling qualitatively confirmed that the BMSCs expressing the shRNA targeting ITGA6 transcripts did not express detectable levels of α6 integrin (Fig. 2C), and consequently, their adhesion to laminin was quantitatively disrupted (Fig. 2B). When these BMSCs with attenuated α6 integrin subunit expression were co-cultured with HUVECs in our fibrin-based sprouting angiogenesis assay, the resulting capillary networks were 80% shorter in terms of total vessel network length after 7 days relative to those co-cultured with BMSCs transduced with the shNT control (Fig 3A, B). On the other hand, HUVECs co-cultured with BMSCs containing the shNT displayed vessel sprouting to the same extent as those co-cultured with wild type BMSCs as controls. These data collectively suggest that knockdown of α6 integrin subunit expression in BMSCs severely limits HUVEC sprouting.

Knockdown of α6 integrin subunit expression in BMSCs disrupts perivascular association, laminin deposition, and αSMA expression

We hypothesized that the α6β1 integrin receptor is essential for BMSCs to occupy the perivascular space and form pericytic associations with the basement membrane. To address this hypothesis, HUVEC-BMSC 3D co-cultures were fixed and stained for αSMA (green), a pericytic marker, and laminin (red) at day 7. Knockdown of α6 integrin expression in the

BMSCs disrupted their ability to associate with the nascent vessels (Fig. 4A-c), and resulted in very low expression of αSMA and poor laminin deposition around the periphery of the vessel structures. Conversely, both wild type BMSCs and those expressing the shNT constructs exhibited relatively high expression levels of αSMA and readily associated with the laminin-rich basement membrane subjacent to the capillary networks (Fig. 4A-a,b). The absence of BMSCs entirely resulted in no sprouting in this model system (Fig. 4A-d)

To validate the observed effects on laminin, lysates were generated from the 3D HUVEC-BMSC co-culture model of angiogenesis after 7 days via two different methods and used for Western blot detection of laminin (Fig. 4B). Nattokinase digestion of the gels resulted in cleaner Western results (left) than sonication (right). Regardless, both extraction methods confirmed reduced laminin levels in cultures containing BMSCs with attenuated α6 integrin subunit expression relative to wild type controls.

To quantify the changes in αSMA expression, flow cytometry was used (Fig. 4C). When cultured in 2D, more than 40% of BMSCs expressed αSMA, whereas fewer than 5% of BMSCs embedded in 3D fibrin gels expressed αSMA. Whether cultured on 2D or in 3D fibrin gels, in the absence of HUVECs, the percentage of BMSCs expressing αSMA in the knockdown conditions were comparable to those of the control conditions containing the wild type BMSCs or those expressing the shNT vector. However, when co-cultured with HUVECs in 3D fibrin gels, the number of BMSCs expressing αSMA increased relative to the BMSCs cultured alone in 3D fibrin gels. More importantly, in these HUVEC-BMSC-3D co-cultures, the αSMA expression levels were significantly decreased in the BMSCs whose α6 integrin was knocked down (Fig. 4C). Expression levels of αSMA detected via Western blotting were consistent with the flow cytometry data, confirming that the BMSCs with attenuated α6 integrin expressed lower levels of αSMA when co-cultured with HUVECs in 3D relative to those expressing the shNT or wild type BMSCs (Fig. 4C). Westerns also confirmed elevated expression of αSMA in 2D cultures of BMSCs relative to the low levels of αSMA expression in the BMSCs cultured alone in 3D fibrin gels (Fig. 4C).

Knockdown of α6 integrin subunit expression has a significant inhibitory effect on BMSC proliferation

Fluorescent images of the 3D co-cultures qualitatively showed fewer BMSCs surrounding the HUVEC-derived capillary networks in the knockdown conditions (Fig. 5A-c), suggesting that perhaps the BMSCs with attenuated α6 integrin proliferated at a slower rate relative to wild type BMSCs or those containing the shNT construct (Fig. 5A-a,b). This was quantitatively confirmed via the total DNA extracted from cells at discrete time points as a measure of cell proliferation over the 7 day culture period (Fig. 5B,C). Cultured in 3D fibrin gels, in the absence of HUVECs, the BMSCs with attenuated α6 integrin proliferated approximately 40% less than either control cells expressing the shNT or wild type BMSCs, indicating that knockdown of α6 integrin significantly reduces the proliferation of BMSCs in 3D fibrin gels (Fig. 5B). In co-culture with HUVECs, similar reductions in proliferation were observed, with the total levels of DNA higher due to the presence of the HUVECs (Fig. 5C). To compensate for this deficit in proliferation, the sprouting angiogenesis assay was repeated with the initial seeding density of ITGA6 knock-down BMSCs increased from 5×10^4 cells/gel to 9.5×10^4 cells/gel in the HUVEC-BMSC co-cultures. Despite the presence of additional BMSCs to normalize for cell number, a significant deficiency in sprouting was still evident (Fig. 6A). These data suggest that decreased vessel formation is not solely the result of the deficit in BMSC proliferation.

BMSCs lacking the α6 integrin receptor are still capable of promoting a baseline vessel sprouting when overlaid as a monolayer on top of the fibrin gels

To further examine the apparent role of α6 integrin knockdown in deficient HUVEC sprouting, BMSCs were seeded on top of the 3D fibrin constructs, rather than distributed throughout the EC-containing gels. This co-culture method has been previously used to effectively isolate the ECs from the stromal support cells in order to explore the effects of soluble, diffusive factors [21, 26, 33]. This assay format was used here to determine if proximity between the HUVECs and BMSCs played a role in the α6 integrin-dependency of angiogenic sprouting. With this altered configuration, the BMSCs with attenuated α6 integrin expression stimulated the HUVECs to sprout to the same extent as either wild type BMSCs or those containing the shNT construct, with no significant differences observed across the conditions (Fig. 7A). Fluorescent images of mCherry-expressing HUVECs at day 7 qualitatively support the quantitative data (Fig. 7B). These data suggest that knockdown of the α6 integrin in BMSCs does not adversely affect their ability to secrete a baseline level of soluble pro-angiogenic cues, but rather that the α6 integrin plays a significant role in regulating the enhanced angiogenic sprouting observed when HUVECs and BMSCs reside in close proximity.

Discussion

It is widely recognized that BMSCs are capable of inducing angiogenesis, and may exert a significant fraction of their therapeutic benefits in this manner. However, the mechanisms underlying their angiogenic capacities remain largely unknown. While there has been much focus on their ability to secrete soluble paracrine factors [34, 35], here we explored a different possibility building on prior studies showing that adult progenitor cells express the laminin receptor α6β1 integrin, and that this integrin may be involved in their perivascular association [17, 23]. We used RNA interference and a HUVEC-BMSC co-culture model of angiogenesis to demonstrate that the α6 integrin subunit is a critical regulator of the ability of BMSCs to promote capillary morphogenesis. When BMSCs were distributed around HUVEC-coated beads in 3D fibrin gels, knockdown of their α6 integrin subunit severely restricted their ability to induce HUVEC sprouting, disrupted their association with nascent vessels, altered their expression of αSMA, and inhibited their proliferation. Knockdown of this integrin also appeared to reduce laminin expression and deposition in the vascular basement membrane. Furthermore, experiments in which BMSCs were cultured as a monolayer a fixed distance away from the HUVECs also suggest that knockdown of α6 integrin expression does not impair the ability of BMSCs to secrete paracrine mediators of angiogenesis. Collectively, these findings show that the α6 integrin subunit on BMSCs plays a critical role in their ability to stimulate an angiogenic response.

Vascular pericytes serve as stabilizing constituents in the development of nascent vessels, and are distinguished by their intimate association with ECs and the expression of pericyte markers, including αSMA and NG2 [36]. Prior studies have suggested that all MSC populations reside in perivascular niches and may in fact all be pericytes [3, 4, 37]; however, this is not to say that all pericytes are necessarily MSCs. Because of their location adjacent to small blood vessels in most tissues [3], MSCs are physically positioned to make important contributions to blood vessel stabilization and immune system homeostasis under various physiological conditions, and can assume a more active role following tissue injury [4]. In this perivascular niche, they can affect ECs in part via secreted growth factors and cytokines [38], but also perhaps via cadherin-mediated cell-cell interactions and interactions with the vascular basement membrane [36]. The data presented here bring forth the significance of the latter of these possible mechanisms.

Consistent with our previous work [20, 24, 25], we show here that HUVECs coated on microcarrier beads and embedded within 3D fibrin matrices form robust capillary-like networks in the presence of MSCs (Fig. 1). In our previous studies, these types of sprouts were highly characterized, showing that they possess hollow lumens [20] and a basement membrane [20, 23], regulate their own permeability [10], and can inosculate with host vessels upon *in vivo* implantation, even when initiated from microcarrier beads [21] By contrast, in the absence of MSCs, the HUVECs failed to sprout (Fig. 3A-d). Therefore, this model system provided an ideal platform to assess the putative role of BMSCs' α6β1 integrin in vessel sprouting.

RNA interference was used to attenuate the expression of α6 integrin subunit in BMSCs (Fig. 2). When used in our assay, these BMSCs were able to induce HUVEC sprouting to levels that were only about 20% of those induced by control BMSCs (Fig. 3). Attenuation of α6 integrin in the BMSCs also led to decreased deposition of laminin around the periphery of the vessel structures (Fig. 4A) and reduced expression of laminin overall in the 3D EC-BMSC co-cultures (Fig. 4B). These findings are consistent with another study, which showed that pericyte recruitment to EC-derived nascent vessels is necessary for vascular basement membrane assembly [39]. In addition, knocking down α6 integrin expression also inhibited BMSC expression of αSMA (Fig. 4B), suggesting that their ability to differentiate into pericytes may depend on this integrin-mediated interaction. Further studies are needed to fully test this possibility since the expression levels of other pericyte markers were not quantified here.

Collectively, the observed effects on BMSC recruitment, αSMA expression, and laminin expression/deposition suggest that the impaired ability of α6 integrin knockdown BMSCs to stimulate vascular morphogenesis may be due to their inability to bind laminin in the vascular basement membrane. However, since we did not perform the reciprocal knockdown of laminin, it is possible that a ligand other than laminin is responsible for the phenotypes observed. Furthermore, we did not investigate which specific isoforms of laminin may be involved, something we hope to be able to do in future studies. One prior study suggested that α6β1 integrin has a broad specificity for multiple laminin isoforms, with a preference for laminin-111, laminin-332, and laminin-511/521 [40]. Of these, laminin-511 is a possible candidate since the laminin α5 chains are expressed by ECs and present in the vascular basement membrane [41]. However, it is not yet clear which, if any, of these laminin isoforms is the ligand for the BMSCs' α6 integrin and mechanistically responsible for the observations reported here.

We also observed that attenuation of the α6 integrin inhibited BMSC proliferation in our fibrin assays, both in the absence and presence of ECs (Fig. 5). This reduced proliferation may be a consequence of the disrupted integrin-laminin interaction or an off-target effect of silencing via RNA interference. Compensating for the reduced numbers of BMSCs in the cultures in which α6 integrin was silenced by seeding a higher number initially still failed to restore sprouting to the levels of wild-type cells (Fig. 6), suggesting that any off-target effects on BMSC proliferation played a minor role in the observed reduction in HUVEC sprouting. Another possibility is that down-regulation of this integrin influences the BMSCs' secretion of soluble pro-angiogenic cues. However, when BMSCs were overlaid on top of fibrin gels a fixed distance away from the HUVEC-coated beads, we showed that capillary sprouting was stimulated equally as well by control BMSCs and those with attenuated α6 integrin (Fig. 7). This result suggests that BMSCs with attenuated α6 integrin are equally capable of secreting soluble pro-angiogenic cues as wild type cells, but the possibility remains that altered juxtacrine signaling between BMSCs and HUVECs at the vascular basement membrane interface may occur downstream of α6β1 integrin. Prior studies have shown the importance of PDGF and EGF signaling in controlling pericyte

recruitment to EC tubes [42], while others have also implicated the sphingosine-1-phosphate [36] and the Notch-Jagged-Delta signaling axes [43]. Although we have not explicitly examined these signaling molecules here, future work can determine if these pathways are influenced, to a degree, by α6β1 integrin or vice-a-versa.

Modulation of α6 integrin levels in BMSCs may also play a role in EC invasion and subsequent vessel formation, in part, by controlling the production of proteolytic enzymes responsible for regulating ECM degradation [44]. In fibrin gels, there have been conflicting reports regarding the relative roles of MMPs [45, 46] and plasmin [47] during EC sprouting, but we recently reported that BMSCs direct HUVECs to sprout in fibrin via a mechanism that exclusively requires the membrane anchored matrix metalloproteinase, MT1-MMP [24]. Furthermore, previous studies in 3D collagen matrices have shown that cross-talk between ECs and pericytes locally regulates EC MT1-MMP expression and/or activity [48], perhaps via EC production of TIMP-3 and pericyte production of TIMP-2 [49, 50]. Therefore, it is possible that the interaction of BMSC α6 integrin with the vascular basement membrane regulates MMP-dependent pathways that control ECM degradation, which in turn influence vessel formation and pericyte differentiation.

In summary, we report the use of an established 3D model of angiogenesis to show that expression of the α6β1 integrin by BMSCs influences their ability to induce endothelial cell capillary tube formation. Down-regulation of the α6 subunit of this integrin via RNA interference resulted in reduced vessel sprouting. Future studies using other stromal cell types may reveal whether the interaction between α6β1 integrin receptor and laminin in the basement membrane is specific to BMSCs, and to what extent this interaction is responsible for the superior quality of vessels achieved by co-delivering HUVECs with BMSCs *in vivo*. [11]

Acknowledgments

We are grateful to Dr. Thomas Lanigan and the University of Michigan Vector Core for technical assistance, and to Dr. Jan Stegemann and Dr. Michael Mayer for providing us access to some key instruments. This work was supported by a grant from the US National Institutes of Health (R21-DE021537).

Abbreviations

3D	three-dimensional
BMSC	bone marrow-derived mesenchymal stem cell
EC	endothelial cell
MSC	mesenchymal stem cell
HUVEC	human umbilical vein endothelial cell
NSC	neural stem cell
αSMA	alpha-smooth muscle actin
NG2	neuron-glial antigen 2
shRNA	small hairpin RNA

References

1. Carmeliet P, Jain RK. Angiogenesis in cancer and other diseases. Nature. 2000; 407(6801):249–57. [PubMed: 11001068]

2. Zandonella C. Tissue engineering: The beat goes on. Nature. 2003; 421(6926):884–6. [PubMed: 12606967]
3. Crisan M, Yap S, Casteilla L, Chen CW, Corselli M, Park TS, Andriolo G, Sun B, Zheng B, Zhang L, Norotte C, Teng PN, Traas J, Schugar R, Deasy BM, Badylak S, Buhring HJ, Giacobino JP, Lazzari L, Huard J, Peault B. A perivascular origin for mesenchymal stem cells in multiple human organs. Cell Stem Cell. 2008; 3(3):301–13. [PubMed: 18786417]
4. da Silva Meirelles L, Caplan AI, Nardi NB. In search of the in vivo identity of mesenchymal stem cells. Stem Cells. 2008; 26(9):2287–99. [PubMed: 18566331]
5. Jain RK. Molecular regulation of vessel maturation. Nat Med. 2003; 9(6):685–93. [PubMed: 12778167]
6. Gerhardt H, Betsholtz C. Endothelial-pericyte interactions in angiogenesis. Cell Tissue Res. 2003; 314(1):15–23. [PubMed: 12883993]
7. McDonald DM, Choyke PL. Imaging of angiogenesis: from microscope to clinic. Nat Med. 2003; 9(6):713–25. [PubMed: 12778170]
8. Cuevas P, Gutierrez-Diaz JA, Reimers D, Dujovny M, Diaz FG, Ausman JI. Pericyte endothelial gap junctions in human cerebral capillaries. Anat Embryol (Berl). 1984; 170(2):155–9. [PubMed: 6517350]
9. Hall AP. Review of the pericyte during angiogenesis and its role in cancer and diabetic retinopathy. Toxicol Pathol. 2006; 34(6):763–75. [PubMed: 17162534]
10. Grainger SJ, Putnam AJ. Assessing the permeability of engineered capillary networks in a 3D culture. PLoS One. 2011; 6(7):e22086. [PubMed: 21760956]
11. Grainger SJ, Carrion B, Ceccarelli J, Putnam AJ. Stromal Cell Identity Influences the In Vivo Functionality of Engineered Capillary Networks Formed by Co-delivery of Endothelial Cells and Stromal Cells. Tissue Eng Part A. 2013
12. Hauner H, Schmid P, Pfeiffer EF. Glucocorticoids and insulin promote the differentiation of human adipocyte precursor cells into fat cells. J Clin Endocrinol Metab. 1987; 64(4):832–5. [PubMed: 3546356]
13. Grigoriadis AE, Heersche JN, Aubin JE. Differentiation of muscle, fat, cartilage, and bone from progenitor cells present in a bone-derived clonal cell population: effect of dexamethasone. J Cell Biol. 1988; 106(6):2139–51. [PubMed: 3384856]
14. Ferrari G, Cusella-De Angelis G, Coletta M, Paolucci E, Stornaiuolo A, Cossu G, Mavilio F. Muscle regeneration by bone marrow-derived myogenic progenitors. Science. 1998; 279(5356): 1528–30. [PubMed: 9488650]
15. Caplan AI. All MSCs are pericytes? Cell Stem Cell. 2008; 3(3):229–30. [PubMed: 18786406]
16. Shen Q, Goderie SK, Jin L, Karanth N, Sun Y, Abramova N, Vincent P, Pumiglia K, Temple S. Endothelial cells stimulate self-renewal and expand neurogenesis of neural stem cells. Science. 2004; 304(5675):1338–40. [PubMed: 15060285]
17. Shen Q, Wang Y, Kokovay E, Lin G, Chuang SM, Goderie SK, Roysam B, Temple S. Adult SVZ stem cells lie in a vascular niche: a quantitative analysis of niche cell-cell interactions. Cell Stem Cell. 2008; 3(3):289–300. [PubMed: 18786416]
18. Tavazoie M, Van der Veken L, Silva-Vargas V, Louissaint M, Colonna L, Zaidi B, Garcia-Verdugo JM, Doetsch F. A specialized vascular niche for adult neural stem cells. Cell Stem Cell. 2008; 3(3):279–88. [PubMed: 18786415]
19. Kiel MJ, Morrison SJ. Uncertainty in the niches that maintain haematopoietic stem cells. Nat Rev Immunol. 2008; 8(4):290–301. [PubMed: 18323850]
20. Ghajar CM, Blevins KS, Hughes CC, George SC, Putnam AJ. Mesenchymal stem cells enhance angiogenesis in mechanically viable prevascularized tissues via early matrix metalloproteinase upregulation. Tissue Eng. 2006; 12(10):2875–88. [PubMed: 17518656]
21. Ghajar CM, Chen X, Harris JW, Suresh V, Hughes CC, Jeon NL, Putnam AJ, George SC. The effect of matrix density on the regulation of 3-D capillary morphogenesis. Biophys J. 2008; 94(5): 1930–41. [PubMed: 17993494]
22. Au P, Tam J, Fukumura D, Jain RK. Bone marrow-derived mesenchymal stem cells facilitate engineering of long-lasting functional vasculature. Blood. 2008; 111(9):4551–8. [PubMed: 18256324]

23. Carrion B, Huang CP, Ghajar CM, Kachgal S, Kniazeva E, Jeon NL, Putnam AJ. Recreating the perivascular niche ex vivo using a microfluidic approach. Biotechnol Bioeng. 2010; 107(6):1020–8. [PubMed: 20672286]
24. Kachgal S, Carrion B, Janson IA, Putnam AJ. Bone marrow stromal cells stimulate an angiogenic program that requires endothelial MT1-MMP. J Cell Physiol. 2012; 227(11):3546–55. [PubMed: 22262018]
25. Ghajar CM, Kachgal S, Kniazeva E, Mori H, Costes SV, George SC, Putnam AJ. Mesenchymal cells stimulate capillary morphogenesis via distinct proteolytic mechanisms. Exp Cell Res. 2010; 316(5):813–25. [PubMed: 20067788]
26. Nakatsu MN, Sainson RC, Aoto JN, Taylor KL, Aitkenhead M, Perez-del-Pulgar S, Carpenter PM, Hughes CC. Angiogenic sprouting and capillary lumen formation modeled by human umbilical vein endothelial cells (HUVEC) in fibrin gels: the role of fibroblasts and Angiopoietin-1. Microvasc Res. 2003; 66(2):102–12. [PubMed: 12935768]
27. Nehls V, Drenckhahn D. A novel, microcarrier-based in vitro assay for rapid and reliable quantification of three-dimensional cell migration and angiogenesis. Microvasc Res. 1995; 50(3): 311–22. [PubMed: 8583947]
28. Nakatsu MN, Hughes CC. An optimized three-dimensional in vitro model for the analysis of angiogenesis. Methods Enzymol. 2008; 443:65–82. [PubMed: 18772011]
29. Kachgal S, Carrion B, Janson IA, Putnam AJ. Bone marrow stromal cells stimulate an angiogenic program that requires endothelial MT1-MMP. J Cell Physiol. 2012
30. Schmittgen TD, Lee EJ, Jiang J, Sarkar A, Yang L, Elton TS, Chen C. Real-time PCR quantification of precursor and mature microRNA. Methods. 2008; 44(1):31–8. [PubMed: 18158130]
31. Carrion B, Janson IA, PKong Y, Putnam AJ. A Safe and Efficient Method to Retrieve Mesenchymal Stem Cells from Three-Dimensional Fibrin Gels. Tissue Eng Part C Methods. 2013
32. Kniazeva E, Kachgal S, Putnam AJ. Effects of extracellular matrix density and mesenchymal stem cells on neovascularization in vivo. Tissue Eng Part A. 2011; 17(7–8):905–14. [PubMed: 20979533]
33. Griffith CK, Miller C, Sainson RC, Calvert JW, Jeon NL, Hughes CC, George SC. Diffusion limits of an in vitro thick prevascularized tissue. Tissue Eng. 2005; 11(1–2):257–66. [PubMed: 15738680]
34. Caplan AI, Correa D. The MSC: an injury drugstore. Cell Stem Cell. 2011; 9(1):11–5. [PubMed: 21726829]
35. da Meirelles LS, Fontes AM, Covas DT, Caplan AI. Mechanisms involved in the therapeutic properties of mesenchymal stem cells. Cytokine Growth Factor Rev. 2009; 20(5–6):419–27. [PubMed: 19926330]
36. Armulik A, Abramsson A, Betsholtz C. Endothelial/pericyte interactions. Circ Res. 2005; 97(6): 512–23. [PubMed: 16166562]
37. Covas DT, Panepucci RA, Fontes AM, Silva WA Jr, Orellana MD, Freitas MC, Neder L, Santos AR, Peres LC, Jamur MC, Zago MA. Multipotent mesenchymal stromal cells obtained from diverse human tissues share functional properties and gene-expression profile with CD146+ perivascular cells and fibroblasts. Exp Hematol. 2008; 36(5):642–54. [PubMed: 18295964]
38. Gnecchi M, Zhang Z, Ni A, Dzau VJ. Paracrine mechanisms in adult stem cell signaling and therapy. Circ Res. 2008; 103(11):1204–19. [PubMed: 19028920]
39. Stratman AN, Malotte KM, Mahan RD, Davis MJ, Davis GE. Pericyte recruitment during vasculogenic tube assembly stimulates endothelial basement membrane matrix formation. Blood. 2009; 114(24):5091–101. [PubMed: 19822899]
40. Nishiuchi R, Takagi J, Hayashi M, Ido H, Yagi Y, Sanzen N, Tsuji T, Yamada M, Sekiguchi K. Ligand-binding specificities of laminin-binding integrins: a comprehensive survey of laminin-integrin interactions using recombinant alpha3beta1, alpha6beta1, alpha7beta1 and alpha6beta4 integrins. Matrix Biol. 2006; 25(3):189–97. [PubMed: 16413178]
41. Yousif LF, Di Russo J, Sorokin L. Laminin isoforms in endothelial and perivascular basement membranes. Cell Adh Migr. 2013; 7(1):101–10. [PubMed: 23263631]

42. Stratman AN, Schwindt AE, Malotte KM, Davis GE. Endothelial-derived PDGF-BB and HB-EGF coordinately regulate pericyte recruitment during vasculogenic tube assembly and stabilization. Blood. 2010; 116(22):4720–30. [PubMed: 20739660]

43. Holderfield MT, Hughes CC. Crosstalk between vascular endothelial growth factor, notch, and transforming growth factor-beta in vascular morphogenesis. Circ Res. 2008; 102(6):637–52. [PubMed: 18369162]

44. Basbaum CB, Werb Z. Focalized proteolysis: spatial and temporal regulation of extracellular matrix degradation at the cell surface. Curr Opin Cell Biol. 1996; 8(5):731–8. [PubMed: 8939664]

45. Hiraoka N, Allen E, Apel IJ, Gyetko MR, Weiss SJ. Matrix metalloproteinases regulate neovascularization by acting as pericellular fibrinolysins. Cell. 1998; 95(3):365–77. [PubMed: 9814707]

46. Lafleur MA, Handsley MM, Knauper V, Murphy G, Edwards DR. Endothelial tubulogenesis within fibrin gels specifically requires the activity of membrane-type-matrix metalloproteinases (MT-MMPs). J Cell Sci. 2002; 115(Pt 17):3427–38. [PubMed: 12154073]

47. Kroon ME, Koolwijk P, van Goor H, Weidle UH, Collen A, van der Pluijm G, van Hinsbergh VW. Role and localization of urokinase receptor in the formation of new microvascular structures in fibrin matrices. Am J Pathol. 1999; 154(6):1731–42. [PubMed: 10362798]

48. Yana I, Sagara H, Takaki S, Takatsu K, Nakamura K, Nakao K, Katsuki M, Taniguchi S, Aoki T, Sato H, Weiss SJ, Seiki M. Crosstalk between neovessels and mural cells directs the site-specific expression of MT1-MMP to endothelial tip cells. J Cell Sci. 2007; 120(Pt 9):1607–14. [PubMed: 17405818]

49. Lafleur MA, Forsyth PA, Atkinson SJ, Murphy G, Edwards DR. Perivascular cells regulate endothelial membrane type-1 matrix metalloproteinase activity. Biochemical and biophysical research communications. 2001; 282(2):463–73. [PubMed: 11401482]

50. Saunders WB, Bohnsack BL, Faske JB, Anthis NJ, Bayless KJ, Hirschi KK, Davis GE. Coregulation of vascular tube stabilization by endothelial cell TIMP-2 and pericyte TIMP-3. J Cell Biol. 2006; 175(1):179–91. [PubMed: 17030988]

Highlights

- BMSCs stimulate angiogenesis, but the mechanisms remain unclear.
- We silenced the expression of the α6 integrin subunit in BMSCs.
- Silencing this receptor subunit significantly inhibited angiogenic sprouting.
- Knocking down α6 integrin affected laminin and αSMA expression.
- Silencing α6 integrin expression also reduced BMSC proliferation.

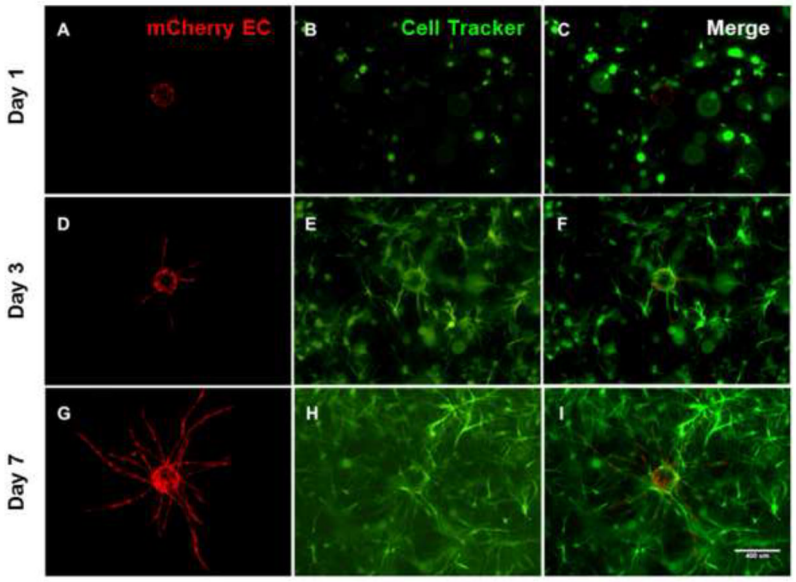

Fig 1. HUVECs recapture their *in vivo* angiogenic capacity in the presence of BMSCs when cultured within three-dimensional fibrin gels

mCherry-transduced HUVECs coated on microcarrier beads were cultured within 2.5 mg/ml fibrin hydrogels in the presence of BMSCs fluorescently labeled using a green cell tracker dye, and their sprouting imaged at day 1 (top row), day 3 (middle row), and day 7 (bottom row). HUVECs (red, panels A, D, G), BMSCs (green, panels B, E, H), and merged channels (C, F, I) are shown. Scale bar = 400 μm.

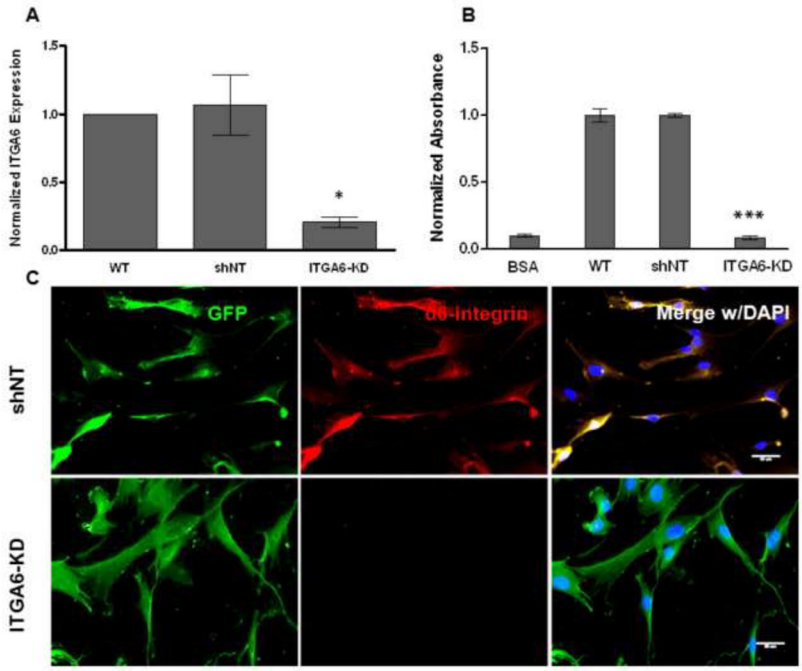

Fig 2. α6 integrin subunit expression was successfully attenuated in BMSCs

A: Expression levels of ITGA6 in BMSCs after knockdown were assessed from three independent experiments via qPCR relative to non-targeting (NT) shRNA controls. * denotes statistical significance ($p < 0.05$) with respect to the scrambled control (shNT). A 2-way ANOVA followed by post-test analyses using Bonferroni's method was used to compare conditions. B: Adhesion of BMSCs onto laminin coated surfaces was disrupted via knockdown of α6 integrin. Adhesion of MSCs with silenced α6 integrin to laminin-coated surfaces was quantified using a crystal violet assay. Raw data generated as absorbance values were normalized to control conditions (adhesion to laminin, blocked with BSA) to correspond to the relative numbers of attached cells in various conditions. *** refers to $p < 0.0001$ with respect to the scrambled control (shNT). C: The expression of α6 integrin subunit (red) was visualized in GFP-expressing BMSCs transduced with non-targeting shRNA (shNT), but was not detectable in BMSCs with silenced α6 integrin (ITGA6-KD). Fluorescent images were taken 1 day following cell seeding. In overlay images, cell nuclei are stained with DAPI (blue). Scale bar = 50 μm.

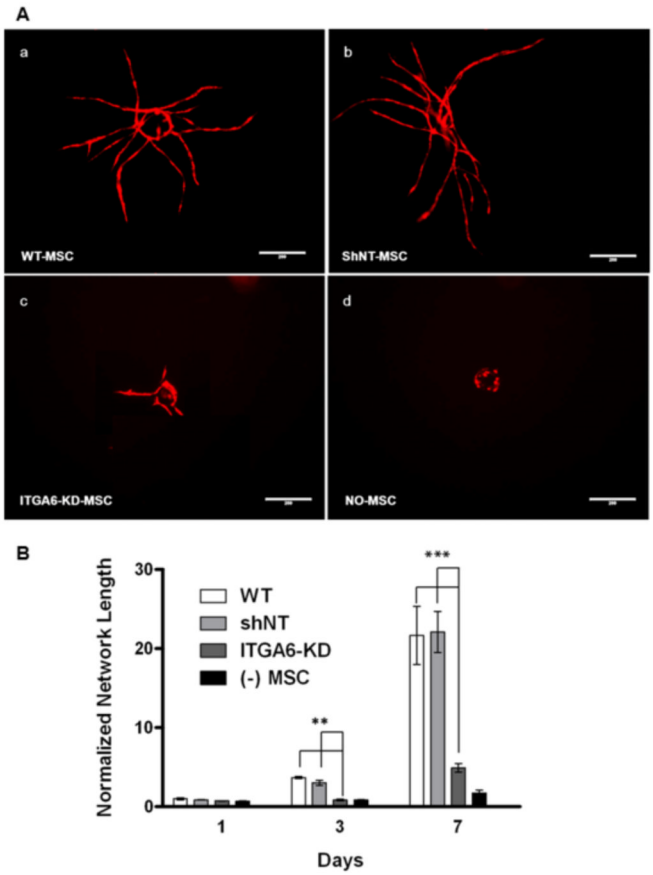

Fig 3. Knockdown of α6 integrin subunit expression in BMSCs diminishes vessel sprouting

A: Day 7 fluorescent images of mCherry-expressing HUVECs co-cultured with (a) wild type BMSCs, (b) BMSCs transduced with non-targeting (NT) shRNA, (c) BMSCs with shRNA against ITGA6 or (d) no BMSCs. Scale bar = 200 μm. B: Total vessel network lengths were quantified from a minimum of 7 fluorescent images over three independent experiments and normalized by day 1 wild type BMSC condition. *** refers to $p \leq 0.001$ with respect to the non-targeting (shNT) and wild type controls in the same group. A 2-way ANOVA followed by post-test analysis using Bonferroni's method was used to compare conditions.

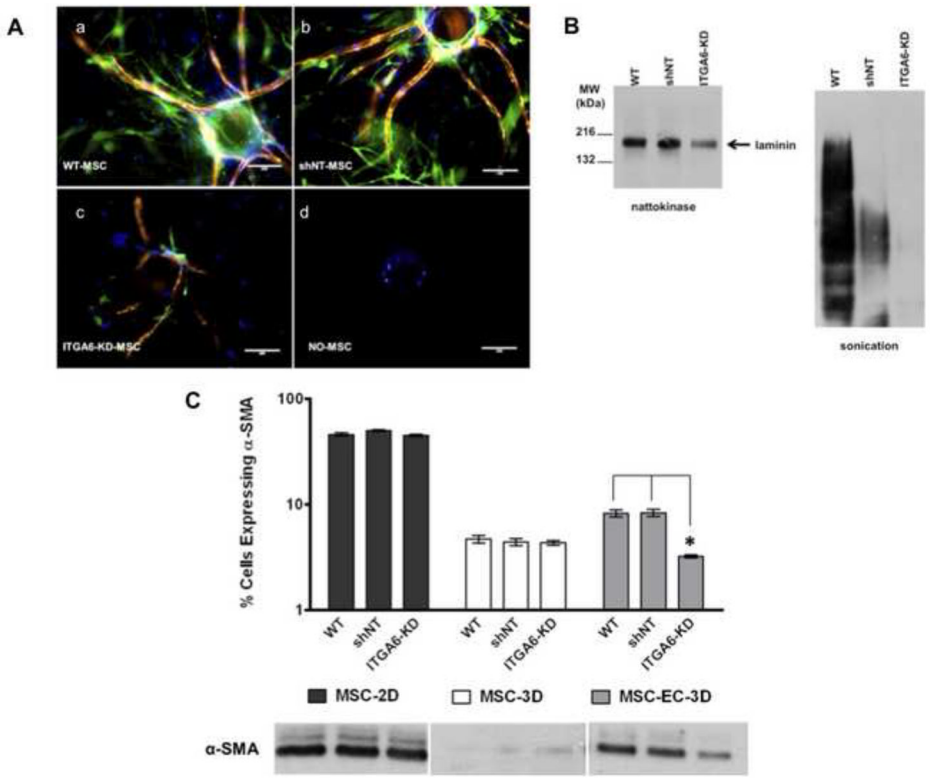

Fig 4. BMSCs with attenuated α6 integrin expression exhibit reduced association with vessel networks, disrupt laminin expression, and express reduced levels of αSMA

A: Representative immunofluorescent images from day 7 3D co-cultures with HUVECs cultured on microcarrier beads in the presence of (a) wild type BMSCs (WT), (b) BMSCs transduced with non-targeting (NT) shRNA (shNT), (c) BMSCs with silenced α6 integrin (ITGA6-KD), or (d) no BMSCs. Cultures were stained for laminin (red), alpha smooth muscle actin (αSMA, green), and nuclei (DAPI, blue). Scale bar = 200 μm. B: Western blot analysis of laminin from lysates generated from 3D fibrin-based models of angiogenic sprouting after 7 days of culture. Lysates were generated either via nattokinase digestion of the fibrin matrix (left), or via sonication to break apart the fibrin (right). Blots were probed with a pan-laminin antibody that reacts with all laminin isoforms. C: Flow cytometric analysis of αSMA expression in WT, shNT, and ITGA6-knockdown BMSCs. Graph shows the percentage (%) of BMSCs expressing αSMA retrieved from day 7 HUVEC-BMSC co-cultures in three independent experiments. Western blot analysis of αSMA expression in BMSCs as a function of culture condition (3D with HUVECs, in 3D without HUVECs, and in 2D without HUVECs) qualitatively confirmed the quantitative flow cytometry results.

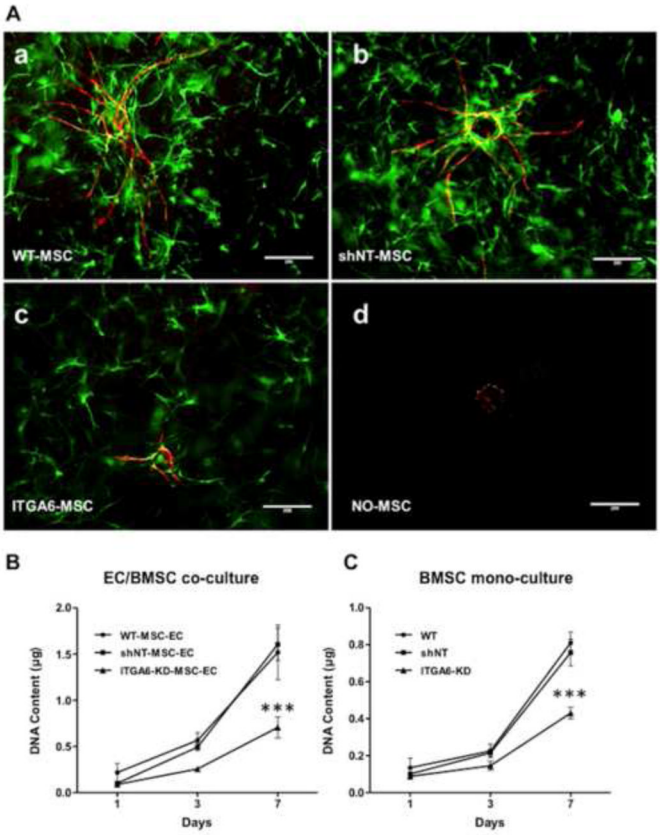

Fig 5. BMSCs with attenuated α6 integrin expression proliferate significantly less than control cells expressing the shNT or wild type BMSCs

A: Representative immunofluorescent images from day 7 3D co-cultures with mCherry-expressing HUVECs cultured on microcarrier beads in the presence of (a) wild type BMSCs tagged with a green cell tracker dye (WT), GFP-expressing (b) BMSCs transduced with non-targeting (NT) shRNA (shNT), (c) BMSCs with silenced α6 integrin (ITGA6-KD), or (d) no BMSCs. B, C: The total DNA extracted from HUVEC/BMSC co-cultures (B) or from BMSC mono-cultures (C) in 3D fibrin gels was assessed as a measure of cell proliferation over a 7 day culture period. *** refers to $p \leq 0.001$ relative to the wild-type and shNT controls (n=3).

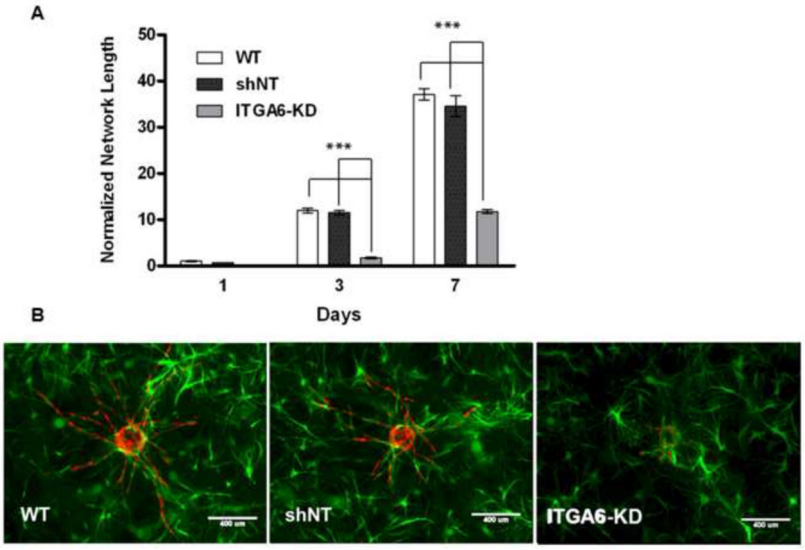

Fig 6. Addition of the BMSCs with attenuated α6 integrin does not compensate for sprouting deficiency in the knockdown conditions

A: Total vessel network lengths were quantified from a minimum of 7 fluorescent images over three independent experiments and normalized by day 1 wild type BMSC condition. *** refers to $p \leq 0.001$ in comparison to the respective non-targeting control in the same group. A 2-way ANOVA followed by post-test analysis using Bonferroni's method was used to compare group conditions. B: Day 7 fluorescent images of mCherry-expressing HUVECs co-cultured with GFP-expressing (a) wild type BMSCs, (b) BMSCs transduced with non-targeting (NT) shRNA, (c) BMSCs with shRNA against ITGA6 (ITGA6-KD). Scale bar = 400 μm.

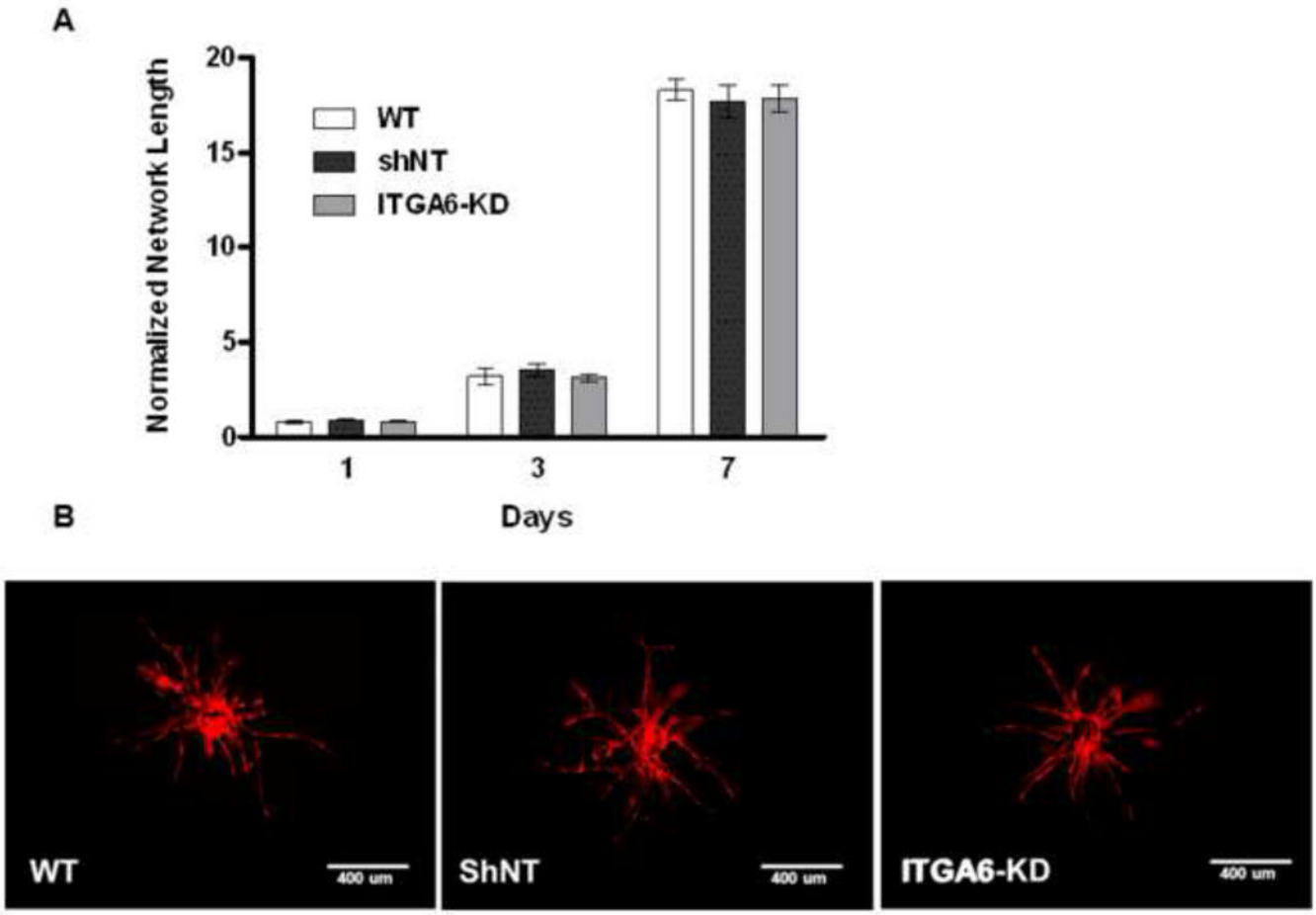

Fig 7. Knockdown of α6 integrin in BMSCs does not limit their ability to support angiogenic sprouting when cultured as a monolayer on top of 3D fibrin

A: Total vessel network lengths were quantified from a minimum of 7 fluorescent images over three independent experiments and normalized by day 1 wild type BMSC condition. B: Representative day 7 fluorescent images of mCherry-expressing HUVECs cultured within fibrin gels overlaid with (a) wild type BMSCs, (b) BMSCs transduced with the non-targeting (NT) shRNA, or (c) BMSCs with shRNA against ITGA6 (ITGA6-KD). Scale bar = 400 μm.